IET Nanobiotechnology

Research Article

IET Journals
The Institution of Engineering and Technology

Green synthesis of anisotropic gold nanoparticles using hordenine and their antibiofilm efficacy against *Pseudomonas aeruginosa*

ISSN 1751-8741
Received on 20th March 2017
Revised 21st June 2017
Accepted on 4th July 2017
E-First on 5th October 2017
doi: 10.1049/iet-nbt.2017.0069
www.ietdl.org

Jobina Rajkumari[1], Himani Meena[1], Muralitharan Gangatharan[2], Siddhardha Busi[1] ✉

[1]*Department of Microbiology, School of Life Sciences, Pondicherry University, Puducherry 605014, India*
[2]*Department of Microbiology, School of Life Sciences, Bharathidasan University, Tiruchirappalli 620024, India*
✉ *E-mail: siddhardha.busi@gmail.com*

Abstract: *Pseudomonas aeruginosa* is a notorious pathogen that causes biofilm aided infections in patients with cystic fibrosis and burn wounds, resulting in significant mortality in immunocompromised individuals. This study reports a novel one-step biosynthesis of gold nanoparticles using phytocompound, hordenine (HD), as a reducing and capping agent. The synthesis of the anisotropic hordenine-fabricated gold nanoparticles (HD-AuNPs) with an average particle size of 136.87 nm was achieved within 12 h of incubation at room temperature. Both HD and HD-AuNPs exhibited significant antibiofilm activity against *P. aeruginosa* PAO1, although greater biofilm inhibition was observed for the nanoparticles as compared to hordenine alone. In the microtitre plate assay and tube method, the nanoparticles significantly inhibited the biofilm formation by 73.69 and 78.41%, respectively. The exopolysaccharide production by the test pathogen was arrested by 68.46% on treatment with the nanoparticles. Further, the effect of HD and HD-AuNPs on the biofilm architecture of *P. aeruginosa* was revealed by light and confocal laser-scanning microscopy micrographs. The overall results of this study suggested the synergistic antibiofilm effect of AuNPs and HD for the treatment of chronic bacterial infections caused by biofilms forming pathogens.

1 Introduction

Microbial biofilms account for many acute as well as chronic infections. Due to their inherent tolerance to antimicrobial agents, they contribute to the development of biofilm-specific antimicrobial resistance in clinical isolates. *Pseudomonas aeruginosa*, an opportunistic human pathogen, takes advantage of its biofilm growth in causing diseases in the patient suffering from cystic fibrosis, chronic wound infections, chronic otitis media and chronic bacterial prostatitis. *P. aeruginosa* is also responsible for 12% of all hospital-acquired urinary tract infections and infections associated with medical device and surgical implants [1, 2]. Inside the biofilm matrix, the bacteria get enclosed in an exopolymeric matrix that acts as a protective sheet to the hostile environment. In *Pseudomonas* sp., the extracellular polysaccharides (EPS) constitute the major component of the biofilm which aids in the initiation, maintenance and dispersal of the biofilm. In addition, it enhances cell surface and facilitates the intercellular adhesion. Flagella govern the swimming and swarming motility of *P. aeruginosa*. It also acts as an adhesin and aids in the initial attachment of the biofilm to abiotic surfaces [3]. Due to the continuous rise in multi-drug-resistant (MDR) strains and their tolerance towards conventional antibiotics, alternative means to combat the problem of biofilms and biofilm-based infections is urgently required.

Plants are used since time immemorial for the treatment of various diseases. Novel phytocompounds are screened and reported for the biofilm inhibition and eradication of pathogens. Hordenine [4-(2-dimethylaminoethyl)] is a phenethylamine alkaloid found in several plants such as *Anhanolium fissuratus*, *Hordeum vulgare*, cactus and bitter orange. It is also found in red algae *Phyllophora nervosa*, *Ahnfeltia paradoxa*, *Gigartina stellata* and *Gelidium crinale*. Hordenine has long been used for the treatment of diarrhoea and dysentery. It is believed to possess various pharmacological effects, including antibacterial and anti-quorum sensing activity against microorganisms [4, 5]. However, the major challenge in antimicrobial therapy till now is its low bioavailability, short half-life and systemic toxicity [6].

The rapid advancement in the area of nanomedicine has opened new avenues for the clinical application of nanoparticles in the delivery of therapeutic agents, in cancer photodiagnostics, photothermal therapy, as sensors and in the diagnosis of chronic diseases. Antimicrobial properties of diverse nanoparticles of various sizes and shapes have been reported against different MDR pathogens. Owing to their small size and remarkable properties, including optical, magnetic, electronic, and structural properties, they are being used in various applications such as cellular imaging, molecular diagnosis and targeted therapy [7]. Gold nanoparticles of various sizes and shapes have been reported for their potential applications in biomedicine. Gold nanoparticles (AuNPs) displaying low toxicity, high stability, catalytic and antibacterial activities have gained much interest in biomedical sciences [8, 9]. The nanoparticles owing to their small size easily penetrates inside the biofilm matrix, interacts with the targeted cells and acts as an efficient nanocarrier for the delivery of bioactive compounds [10].

In the past two decades, various plant extracts are extensively studied for its ability to synthesise a wide and diverse range of inorganic nanoparticles including metals, metal oxides, and metal sulphides. However, a very few research has been conducted on the synthesis of AuNPs using pure phytocompound. On the other hand, limited reports have been documented on biological activity of hordenine and till date no reports are available on its antimicrobial activity. Hence, in the present study, AuNPs were successfully synthesised using hordenine as a reducing and fabricating agent. Further, the antibiofilm activity of both HD and hordenine-fabricated gold nanoparticles (HD-AuNPs) against *P. aeruginosa* PAO1 was determined.

2 Materials and methods

2.1 Materials

Hordenine (≥97%) was purchased from Sigma-Aldrich. Gold(III) chloride trihydrate ($HAuCl_4 \cdot 3H_2O$, 99.99%), Congo red, crystal violet (0.1%), acridine orange and ethidium bromide were procured from HiMedia Laboratories Pvt Ltd, India. The test pathogen, *P.*

aeruginosa PAO1 (MTCC 2453), used in this study was procured from Microbial Type Culture Collection and Gene Bank (MTCC), IMTECH, Chandigarh, India.

2.2 Synthesis of HD-AuNPs

Initially, 1 mM solution of gold(III) chloride trihydrate ($HAuCl_4$) was prepared in sterile Milli-Q water. The $HAuCl_4$ solution was mixed with equal volume of 1 mM of hordenine (HD) solution and incubated at 37°C with continuous stirring, until the colour of the solution changes. The nanoparticles in the form of pellet were collected by centrifugation at 10,000 rpm for 20 min and washed thrice with milliQ water. The resultant nanoparticles were air-dried and subjected to further characterisation [11].

2.3 Characterisation of HD-AuNPs

Reaction mixture (2 ml) was subsequently withdrawn and the absorption spectrum was recorded in the range of 350–700 nm using a UV–visible spectrophotometer [12]. Fourier transform infrared (FTIR) spectroscopy analysis was carried out to identify the biomolecules responsible for the bio-reduction of the Au^{3+} ions and capping agent AuNPs. For FTIR measurements, 1 mg of air-dried HD-AuNPs was mixed with 100 mg of potassium bromide (KBr) and made into a circular disc. Likewise, an appropriate amount of hordenine was mixed with KBr for the comparative study of the functional groups. The FTIR spectrum was recorded in the range of 450–4000 cm^{-1} at a resolution of 1 cm^{-1} [13]. The synthesised HD-AuNPs (3 ml) in aqueous solution was subjected to dynamic light scattering (DLS) to determine the average size of the particles. DLS measurements were recorded at a scattering angle of 90° and temperature of 25°C [11]. Morphological and quantitative elemental analysis of synthesised HD-AuNPs was carried out using an scanning electron microscopy (SEM) equipped with energy-dispersive X-ray spectroscopy (EDAX). The powdered nanoparticles were applied onto a carbon-coated grid and analysed under low vacuum with an accelerating voltage of 24 kV [12]. The size and morphology of HD-AuNPs was also analysed using a high-resolution transmission electron microscope (HR-TEM). The sample was prepared on a copper grid as droplets, carbon coated and air-dried. The HR-TEM measurements were performed at an accelerating voltage of 200 kV. The crystal structure of HD-AuNPs was analysed using a selected area electron diffraction (SAED) pattern [14].

2.4 Determination of minimum inhibitory concentration and sub-minimum inhibitory concentrations

The minimum inhibitory concentration (MIC) of HD against *P. aeruginosa* was determined with reference to National Committee for Clinical Laboratory Standards (NCCLS) described by Payne *et al.* [15]. Two-fold serial dilutions of HD were made in Mueller–Hinton broth to attain the final concentration ranging from 15.62 to 1000 µg/ml. Overnight culture of *P. aeruginosa* (1×10^5 CFU/ml) was supplemented in each tube and incubated at 37°C for 24 h under continuous agitation. The tubes to which no HD was added serve as positive control. The MIC is considered as the lowest concentration of HD that inhibited visible growth of *P. aeruginosa* PAO1 on overnight incubation. The turbidity of the culture broth was recorded at the wavelength of 600 nm to determine the sub-minimum inhibitory concentration (Sub-MIC) level. The highest concentration of HD that did not affect growth of the test organism based on the quantification of cell density in regular intervals was recorded as the Sub-MIC concentration. All the experiments were executed in triplicates.

2.5 Antibiofilm activity of HD-AuNPs

Prior to all the assays, the test bacteria were grown in Luria Bertani (LB) medium at 37°C until an optical density (OD) of 0.4 was attained at 600 nm. The antibiofilm efficacy of HD and HD-AuNPs at the Sub-MIC concentration was evaluated.

2.5.1 Microtitre plate (MTP) assay: The quantitative biofilm detection method described by Li *et al.* [16] was employed to determine the antibiofilm efficacy of synthesised HD-AuNPs and HD (125 µg/ml) on *P. aeruginosa* PAO1. Overnight culture of the test organism was prepared in Brain heart infusion (BHI) and the OD was adjusted to 0.5 at 600 nm. Individual wells of sterile 96-well flat-bottom polystyrene tissue culture plate were filled with 200 µl of the test culture and cultivated in the presence 125 µg/ml concentration of HD-AuNPs and HD. Wells containing sterile broth medium without HD-AuNPs or HD were used as positive control. The plates were incubated without agitation at 37°C for 24 h. After incubation, the contents of each well were removed and the wells were gently washed thrice with 0.1% phosphate saline buffer (pH 7.2) to remove the planktonic cells. The biofilm formed by the surface adhered cells in the MTP wells was stained with crystal violet (0.1%) solution for 10 min and the excess stain was removed by washing the wells with deionised water. The crystal violet adhered to the biofilm was destained using ethanol–acetone solution (4:1) and the optical intensity was measured at 570 nm using a UV–visible spectrophotometer. All the experiments were performed in triplicate. The antibiofilm activity was described by the percentage of biofilm inhibition, which was calculated as follows:

$$\text{biofilm inhibition}\,(\%) = [1 - (\text{sample OD}_{570} - \text{control OD}_{570})] \times 100$$

2.5.2 Tube method: The quantitative determination of antibiofilm activity was determined based on the method of Ansari *et al.* [17] with slight modifications. The test organism, *P. aeruginosa* PAO1, was grown in tryptic soy broth (TSB) containing 1% glucose, supplemented with 125 µg/ml of HD-AuNPs and HD. After incubation for 24 h at 37°C, the medium was discarded and the tubes were washed with PBS (1%), air-dried and subsequently stained with 0.1% crystal violet for 1 min. The excess stain was subsequently removed by washing the tubes with sterile distilled water. The adhered cells were destained with DMSO and the OD was measured at 570 nm.

2.5.3 Exopolysaccharide (EPS) quantification: The phenol–sulphuric acid method described by Mary and Banu [18] was employed for the quantification of EPS production. *P. aeruginosa* PAO1 was allowed to form biofilm on the surface of cover glass (1 × 1 cm) immersed in LB broth, in the presence of 125 µg/ml of HD-AuNPs and HD. The slides were incubated at 37°C for 18 h, which was followed by washing with 0.5 ml of NaCl (0.9%) and vortexed for 1 min to extract the EPS. The EPS solution obtained was mixed with equal volume of phenol (5%) and five volume of sulphuric acid (99.99%) and incubated in the dark for 1 h. After incubation, the samples were centrifuged at 10,000 rpm for 10 min, thereafter the absorbance of the supernatant collected was measured at 490 nm. A similar control experiment was carried out in the absence of HD-AuNPs and HD. The percentage of EPS production was calculated using the following formula:

$$\text{EPS production}\,(\%) = [\text{Control OD}_{490}\text{--Test OD}_{490}/\text{Control OD}_{490}] \times 100$$

2.5.4 Congo red agar method: The inhibition of biofilm formation was assessed by the Congo red agar (CRA) method following the method described by Ansari *et al.* [17]. Aqueous Congo red dye was prepared, autoclaved separately and added to pre-cooled sterile BHI agar media supplemented with 50 g/l of sucrose and Congo red dye (0.8 g/l). HD-AuNPs and HD (120 µg/ml) were incorporated into the CRA medium and overnight *P. aeruginosa* PAO1 culture was streaked on the surface of the agar medium. The plates were incubated aerobically at 37°C for 48 h and the colour and texture of the colonies formed were observed. BHI agar devoid of HD-AuNPs or HD serves as control.

2.5.5 Swarming assay: Swarming assays were performed to determine the effect of HD and HD-AuNPs on the motility of the

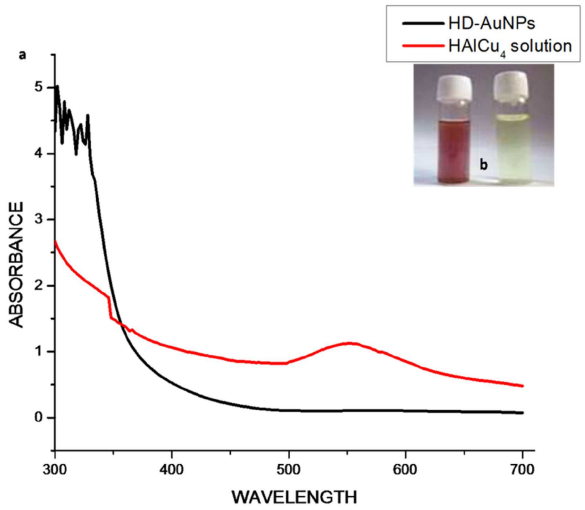

Fig. 1 *Characteristic peak centered*
(a) UV–visible spectra of 1 mM $HAuCl_4$ solution recorded before and after the addition of hordenine, showing maximum intensity peak at 540 nm, ***(b)*** Vials containing 1 mM $HAuCl_4$ solution (right) and HD-AuNPs (left) showing change in colour of the reaction mixture from pale yellow to ruby red

test organism. The freshly grown culture of *P. aeruginosa* PAO1 was point inoculated onto the centre of swarm agar plates comprising of glucose (1%), bacto-agar (0.5%), bacto-peptone (0.6%) and yeast extract (0.2%), in the presence HD and HD-AuNPs (120 µg/ml). The plates were incubated at 37°C for 24 h. Overnight culture of *P. aeruginosa* PAO1 inoculated on the agar plates devoid of HD and HD-AuNPs serves as control. The total distance of bacterial migration from the point of inoculation was recorded to determine the inhibition of bacterial motility [19].

2.5.6 Microscopic observation of biofilm: The effect of HD and HD-AuNPs at a concentration of 125 µg/ml on biofilm formation was analysed using light and confocal laser-scanning microscopy (CLSM). Overnight culture of *P. aeruginosa* PAO1 grown in TSB medium supplemented with glucose (0.5%) was diluted to an OD of 0.5 (OD_{600}) with fresh medium. Briefly, 1% of the cell suspensions were added into 1 ml of fresh growth medium and dispensed into the wells of 12-well microtitre plates containing pre-sterilised cover glasses (13 × 13 mm diameter) along with 125 µg/ml of HD and HD-AuNPs. The plates were statically incubated at 37°C for 24 h. The biofilm formed on the cover glasses in the medium devoid of HD and HD-AuNPs was employed as a control. At the end of incubation, excess stain from the cover glasses was washed off with milliQ water and gently rinsed twice with 0.1% crystal violet dye and observed under a bright-field microscope at 100× magnification [20]. Likewise for the CLSM analysis, the biofilms adhered to the coverslips were stained with 100 µl of acridine orange (0.2%, w/v) and incubated for 10 min in the dark. Thereafter, the coverslips were gently washed twice with PBS to remove the excess stain and visualised under a confocal laser-scanning microscope (Model LSM 710; Carl Zeiss Microscopy GMBH, Germany) at a magnification of 20×. The three-dimensional (3D) images were recorded and Z-stacks were prepared to compare the biofilm thickness and determine the biofilm inhibition efficacy [21].

3 Results and discussion

3.1 Synthesis and characterisation of HD-AuNPs

The change in colour of the solution from pale yellow to ruby red clearly indicated the reduction of Au^{3+} and the formation of HD-AuNPs was observed within 12 h of incubation at room temperature (Fig. 1). The negative control containing $HAuCl_4$ solution did not show any characteristic change in colour. Gold nanoparticles display characteristic colour due to surface plasmon resonance (SPR), resulting from collective excitation of the electrons in the conduction band around the nanoparticle surface. This SPR caused by the oscillating electron induces a strong absorption of the incident light which can be measured using a UV–visible absorption spectrometer. Moreover, the SPR band intensity and wavelength depend on the factors affecting the electron charge density on the particle surface such as metal type, particle size, shape, structure, composition and the dielectric constant of the surrounding medium [7]. The formation of HD-AuNPs was confirmed using UV–Visible spectroscopy where a marked difference was observed between the UV–Visible spectrum of the $HAuCl_4$ solution (control) and HD-AuNPs. A characteristic peak centred at 540 nm, as shown in Fig. 1, was observed due to the excitation of SPR vibration of the gold nanoparticles [14]. Manju *et al.* [8] reported the synthesis of gold nanoparticle using *Nigella sativa* essential oil as a reducing and coating agent, within 30 min of reaction where the UV–vis absorption spectra for AuNPs were recorded at 540 nm. The obtained result was also in agreement with the findings of Sujitha and Kannan [22], who reported the synthesis of AuNPs using aqueous citrus fruits showing a light scattering peak of AuNPs at 550 nm.

The Fourier transformed infrared (FTIR) studies of HD and biosynthesised HD-AuNPs is shown in Fig. 2. The FTIR spectrum of HD showed bands at 2959.97, 2790.83, 2585.83, 1608.24, 1381.29, 1169.37 and 1099.87 cm^{-1} along with few other small bands. A similar FTIR spectrum with a shift in absorption bands at 3427.25, 2919, 2850.76, 1628.68, 1459.69, 1381.17, 1215.6, 1114.06 and 673.11 cm^{-1} was observed in the spectrum of HD-AuNPs. A strong IR band corresponding to N–H stretching vibration of primary amines was observed at 3427.25 cm^{-1}. The bands at 2919 and 2850.76 cm^{-1} correspond to C–H stretching of asymmetry and symmetry vibration, respectively. The medium band at 1628.68 cm^{-1} represents the N–H stretching of amide I band. The absorption bands at 1459.69 and 1215.6 cm^{-1} arise due to the C–C stretching of an aromatic ring and C–N stretching of aliphatic amines, respectively. The IR bands observed at 1381.17 and 1215.6 cm^{-1} represent C–N stretching vibration of aliphatic amine and C–O stretching, respectively. The three bands recorded at 2350.39, 1735.57 and 542.37 cm^{-1} in the spectra of the synthesised nanoparticles represent the (C=O) carbonyl stretching and presence of metal indicating the reduction of gold chloride to AuNPs and binding of HD to Au nanoparticles through the free amine groups or carboxylate ions of the amino acid residues. The presence of functional groups such as amines, alcohol, aldehydes and carboxylic acids also indicates that gold nanoparticles synthesised were fabricated with HD, thereby preventing the aggregation of the nanoparticles and further providing stability [13, 23]. These results recorded were in agreement with earlier reports of Ghosh *et al.* [11], Song *et al.* [12] and Islam *et al.* [23].

The DLS method was employed to calculate the hydrodynamic size of AuNPs coated with the phytocompound. On the DLS analysis, the average diameter of the polydispersed HD-AuNPs was found to be 136.87 nm, as shown in Fig. 3. The EDX pattern, as shown in Fig. 3, showed signature spectra for gold and revealed the highest proportion of Au signals with a high-intensity peak at 2.12 KeV (Fig. 3). Minor peaks of elements such as carbon and oxygen were also observed which could have resulted due to the biomolecules of hordenine bound to the surface of the nanoparticles. Similar EDX spectra were reported previously from the AuNPs synthesised using the extracts of the herb, *Scutellaria barbata* [24]. The SEM micrographs revealed the anisotropic nature of the gold nanoparticles, resembling the shape of flat disc (Fig. 3). The biosynthesised gold nanoparticles presented variable shape, although most of them appeared more or less circular, with a few having occasionally hexagonal shape. The gold nanoparticles displayed a narrow size distribution, with the diameter ranging from 120 to 140 nm. The particle size distribution of the gold nanoparticles determined by the SEM was in good agreement with the DLS analysis. The obtained result was also in accordance with the previous report of Ghosh *et al.* [11], where anisotropic gold nanoparticles with a diameter ranging from 11 to 30 nm were synthesised using tuber extract of *Dioscorea bulbifera*. The SEM micrograph presented polydispersed gold nanoparticles exhibiting

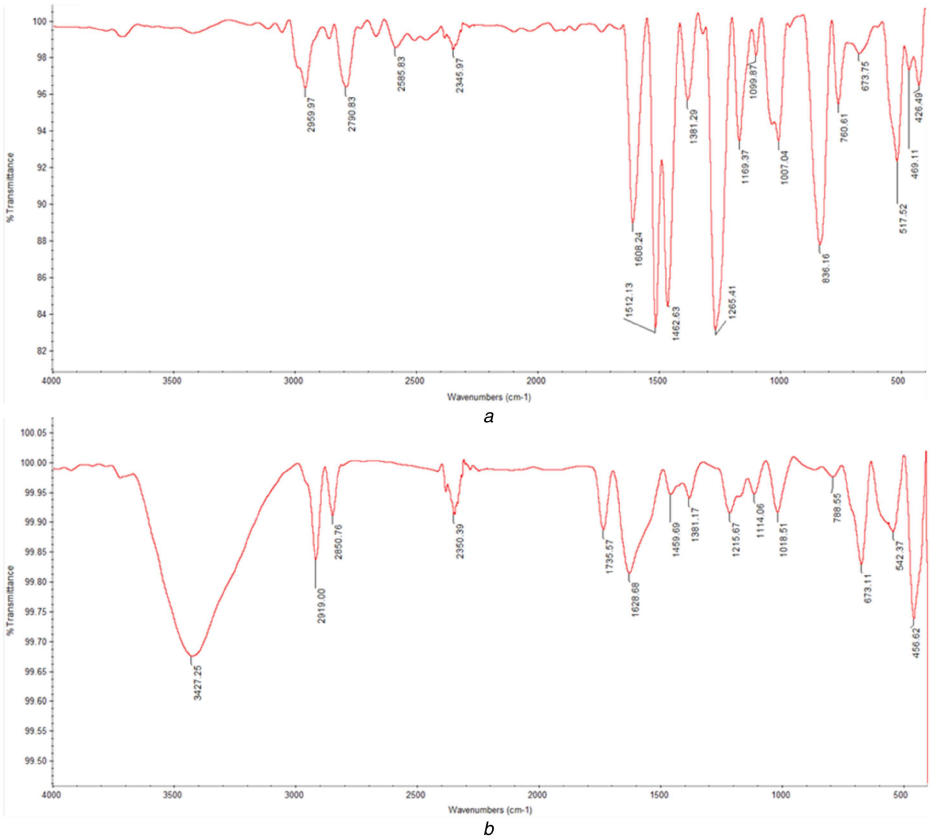

Fig. 2 *FTIR spectra of hordenine and HD-AuNPs synthesised by the reduction of $AuCl_4$ using hordenine. The presence of amines, alcohol, aldehydes and carboxylic acids, functional groups in the FTIR spectra of HD-AuNPs indicated the fabrication of AuNPs by HD*
(a) Hordenine, ***(b)*** HD-AuNPs

variable shape, predominantly spherical with a few triangular in shape [11].

The structure and size of the nanoparticles was further confirmed by the TEM analysis as shown in Fig. 3. The HD-AuNPs were predominantly flat and circular in shape with a size of 130 ± 10 nm in diameter. These findings resemble the anisotropic gold nanoparticles synthesised using *N. sativa* essential oil previously reported by Manju *et al.* [8], where the TEM images exhibited spherical-, triangle- and hexagonal-shaped nanoparticles. Chandran *et al.* [25] also reported the facile synthesis of gold nanotriangles with size ranging from 50 to 350 nm by varying the concentration of Aloe vera leaf extract used in the reduction of the gold ion. The crystalline nature AuNPs was evident from the diffraction pattern on the SAED pattern (Fig. 3). The bright circular rings correspond to the SAED pattern of synthesised Au nanoparticles, showing Debye–Scherrer rings assigned to the (111), (200), (220) and (311) lattice planes of the face-centred cubic (fcc) structure [14]. Similar reports have also been documented by Sujitha and Kannan [22], where citrus fruit-mediated synthesis of crystalline AuNPs was revealed by the typical SAED pattern with bright circular diffraction rings corresponding to the (111), (200), (220) and (311) planes.

3.2 MIC and Sub-MIC

The MIC of HD against *P. aeruginosa* PAO1 was found to be more than 1000 µg/ml and the bacteria growth was found to be significantly inhibited with the increase in the concentration of HD from 250 µg/ml onwards, as compared to the positive control. However, 15.62, 31.25, 62.5 and 125 µg/ml of HD showed no significant difference in the cell density. Hence, 125 µg/ml was considered as the highest Sub-MIC concentration and used as a standard concentration for further antibiofilm assays.

3.3 Antibiofilm activity of HD-AuNPs

3.3.1 MTP assay: As shown in Fig. 4, both HD-AuNPs and HD showed significant antibiofilm inhibition against *P. aeruginosa* PAO1. Although a higher antibiofilm efficacy with an inhibition percentage of 73.69 ± 2.15% was observed on treatment with HD-AuNPs (125 µg/ml) as compared to 63.64 ± 4.4% obtained on treatment with HD (125 µg/ml). Similar biofilm inhibition activity using gum arabic capped-silver nanoparticles was reported by Ansari *et al.* [17] against MDR *P. aeruginosa.*

3.3.2 Tube method: The biofilm formation was significantly reduced in HD-AuNPs (125 µg/ml) treated samples as compared to samples treated with HD (125 µg/ml). The percentage reduction in biofilm formation was found to be 78.41 ± 4.7% in the presence of 125 µg/ml of HD-AuNPs, as shown in Fig. 4. However, on treatment with 125 µg/ml of HD, the decrease in biofilm formation was found to be 68.75 ± 2.87%.

3.3.3 EPS quantification: The EPS matrix provides 1000 times more tolerance to bacteria against antimicrobial agents as compared to planktonic cells, thus resulting in the emergence of MDR bacteria. A significant reduction in EPS production in both HD-AuNPs and HD-treated *P. aeruginosa* PAO1 was observed as shown in Fig. 4. In the presence of HD-AuNPs (125 µg/ml), the decrease in EPS production was found to be 68.46 ± 1.9% while the inhibition of EPS production by 49.34 ± 2.3% was achieved on treatment with 125 µg/ml of HD.

3.3.4 CRA method: The production of EPS is an indispensable part in the formation of biofilm. The EPS constitute the vital part of the biofilm as it encases the planktonic cells inside a protective matrix and provides resistance to external stress. The biofilm inhibition by HD or HD-AuNPs was determined by the reduction of EPS production in *P. aeruginosa* PAO1 on CRA plates. After 48 h of incubation, dark black colonies with crystalline edge were observed on the untreated control plate indicating the production of

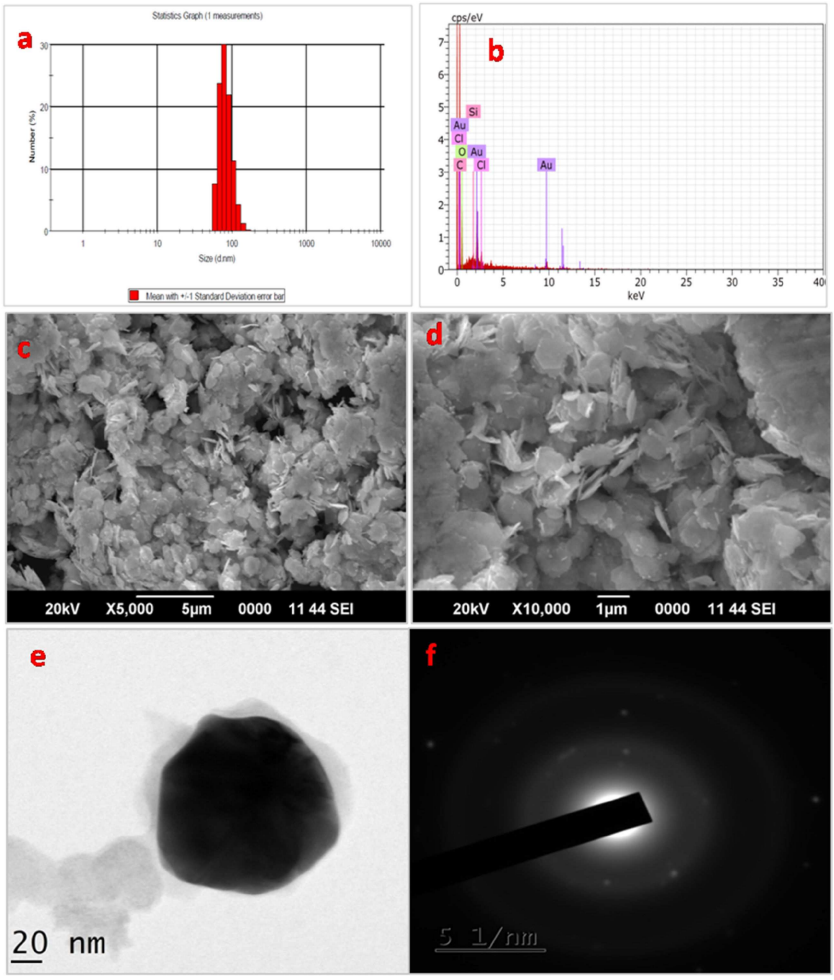

Fig. 3 *The average diameter of the polydispersed HD-AuNPs*

(a) DLS histogram showing particle size distribution of HD-AuNPs, with an average diameter of 136.87 nm, ***(b)*** EDAX graph of HD-AuNPs showing predominant peak of Au along with minor peaks of carbon and oxygen, indicating the presence of hordenine, ***(c, d)*** SEM micrograph of the gold nanoparticles formed by the reaction of 1 mM $HAuCl_4$ and hordenine with a size of 130 ± 10 nm in diameter, ***(e)*** TEM images of the gold nanoparticles showing roughly circular HD-AuNPs, with an average particle diameter of 130 ± 10 nm, ***(f)*** The SAED pattern of the corresponding HD-AuNPs indicating the crystalline nature of the nanoparticles

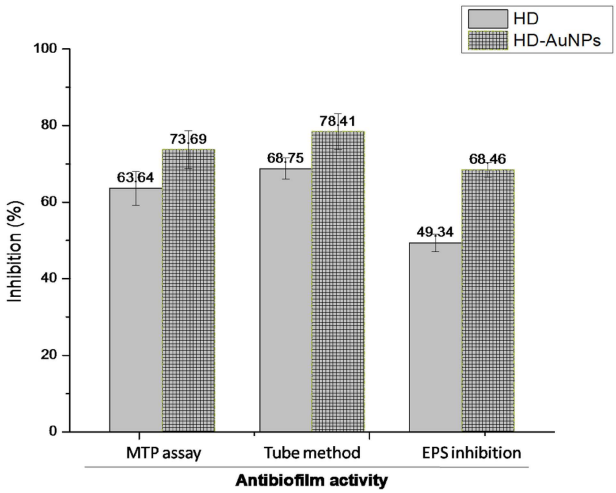

Fig. 4 *Graph showing biofilm inhibition effect of HD and HD-AuNPs (125 µg/ml) determined using microtitre plate assay, tube method and EPS inhibition assay. A higher reduction in biofilm formation of P. aeruginosa PAO1 was exhibited by HD-AuNPs as compared to that of HD*

exopolysaccharides (EPS), as shown in Fig. 5. However, the presence of HD-AuNPs and HD (125 µg/ml) incorporated in the CRA plate significantly arrested the synthesis of EPS, resulting in the formation of pink-coloured colonies [17].

3.3.5 Motility assay: Bacterial motility plays an important role in increasing bacterial colonisation on the abiotic surfaces. HD-AuNPs was further tested for its antagonistic activity against biofilm forming *P. aeruginosa* PAO1 [19]. At 125 µg/ml concentration, HD-AuNPs and HD significantly arrested the bacterial motility when compared to the positive control. The result indicated that HD-AuNPs efficiently controls the flagellum-driven motility of in the test organism (Fig. 5).

3.3.6 Microscopic observation of biofilm: Microscopic analysis of the biofilm was performed to validate the efficacy of HD-AuNPs

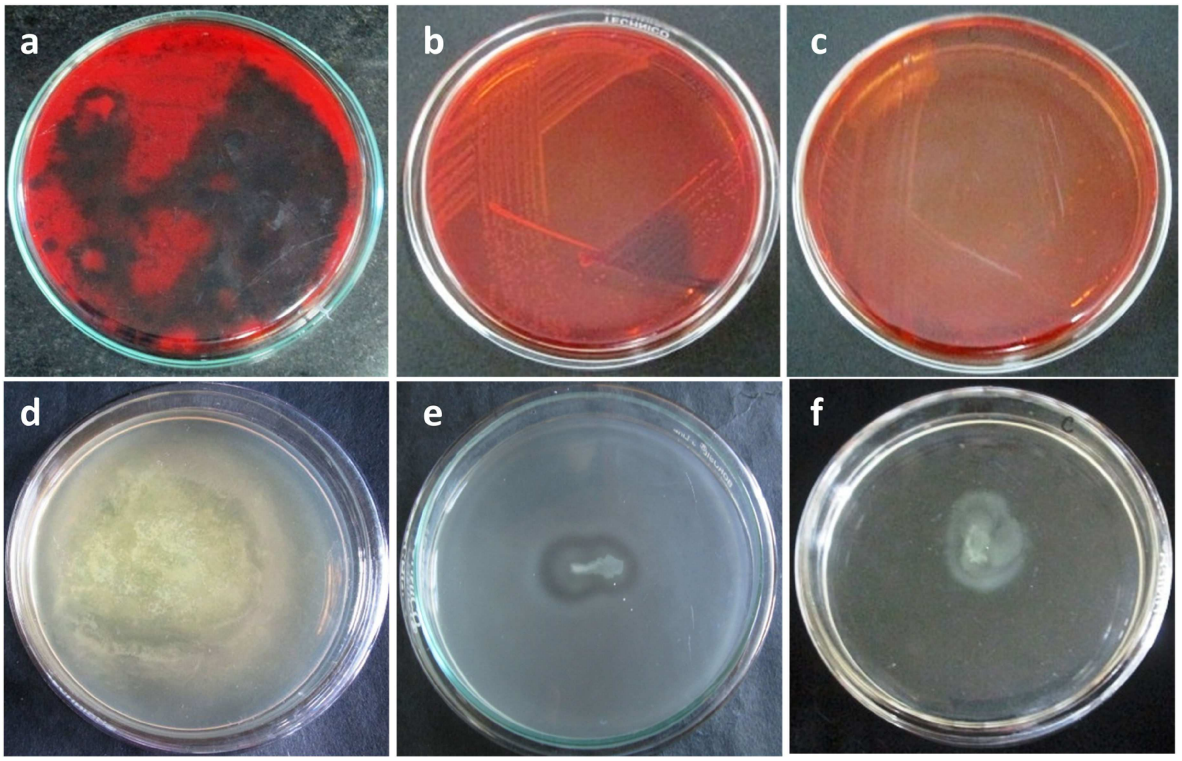

Fig. 5 *Dark black colonies*

(a) Appearance of black crystalline colonies on BHI agar supplemented with Congo red indicating the exopolysaccharide production by *P. aeruginosa* PAO1 (control) and plates showing pink and transparent edged colonies indicates arrest in EPS production in the presence of ***(b)*** HD and ***(c)*** HD-AuNPs (120 µg/ml), decrease in swarming motility of *P. aeruginosa* PAO1 on swarm agar plate on treatment with ***(e)*** HD and ***(f)*** HD-AuNPs (125 µg/ml), as compared to control ***(d)***

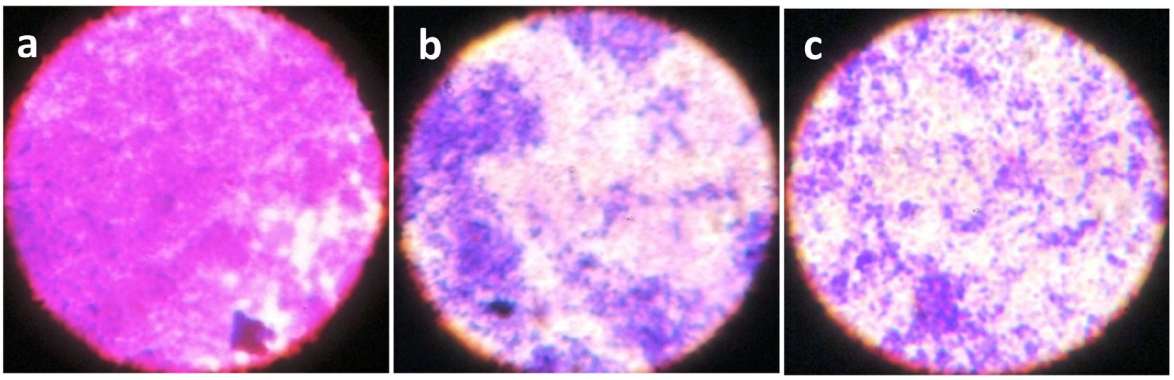

Fig. 6 *Visual evidence of biofilm inhibition showing scattered and dispersed biofilms of P. aeruginosa PAO1, on treatment with 125 µg/ml of HD* ***(b)*** *and HD-AuNPs* ***(c)****, as shown by light microscope images, as compared to control* ***(a)***

and HD as potent biofilm inhibitors. On visualisation of biofilm using a light microscope (Fig. 6) and CLSM (Fig. 7), the biofilm micrographs treated with HD and HD-AuNPs (125 µg/ml) displayed scattered appearance compared to the biofilm formed by untreated *P. aeruginosa* PAO1, after 24 h of incubation. A thick coating of biofilms was observed in control, whereas a visible reduction in numbers of bacterial cells was observed in the biofilms of both HD-treated and HD-AuNPs treated samples.

From the 3D images (*b*, *e* and *h*), it was evident that the thickness of the biofilm was reduced from 80 to 45 µm on treatment with HD, whereas in HD-AuNPs treated biofilm, a higher reduction with a biofilm thickness of 20 µm was obtained. Similar biofilm inhibition activity using gum arabic capped-silver nanoparticles was reported by Ansari *et al.* [17] against MDR *P. aeruginosa.* Thus, the cumulative results suggested the synergistic effect of HD and AuNPs in inhibiting the development of biofilm more efficiently as compared to HD alone. The nano-formulation can also be used towards the development of antimicrobial coatings for medical devices and catheters.

Biofilm provides an ideal environment for the pathogenic bacteria as it blocks the penetration of antimicrobial agents and results in antibiotic resistance. As the biofilm plays an important role in pathogenesis, the inhibition of biofilm formation becomes an important target for therapeutics. Several natural compounds have the potential to interfere with bacterial adherence and formation of biofilm. Gold nanoparticles have been extensively used for biomedical applications, especially for imaging, diagnostic and therapy due to its biocompatibility, non-immunogenicity and non-cytotoxicity. Phytocompound when entrapped in nanoparticles significantly enhances its stability, half-life and bioavailability as compared to free form. In the present study, hordenine was used as a reducing and capping agent for the green synthesis of HD-AuNPs, without thermal assistance. Further, the fabrication of HD to the AuNPs dramatically enhances the antibiofilm activity of HD against *P. aeruginosa* PAO1. Hence, the findings suggested that HD-AuNPs may be exploited towards the development of potential antimicrobial coatings for various medical devices, wound dressing and in the treatment of biofilm-based infections.

4 Conclusion

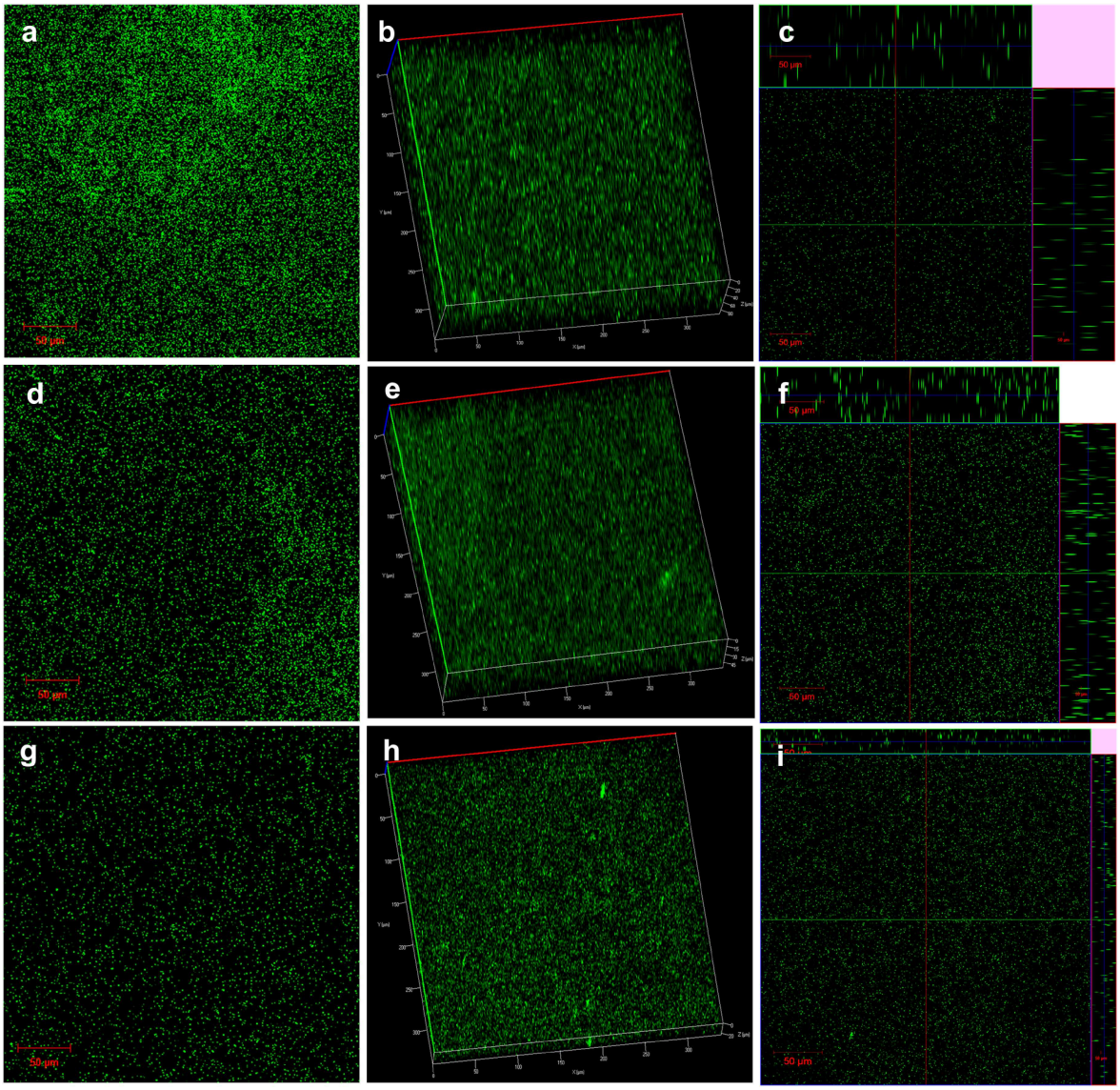

Fig. 7 *2D (**a**, **d**, **g**) and 3D (**b**, **c**, **e**) confocal laser-scanning microscopic images of P. aeruginosa PAO1biofilms (**a**–**c**) untreated controls, (**d**–**f**) HD-treated and (**g**–**i**) HD-AuNPs treated (scale bars = 50 µm)*

5 Acknowledgments

The authors extend their sincere appreciation to Central Instrumentation Facility (CIF), Pondicherry University for extending DLS facility and also Department of Chemistry, Pondicherry University for providing the facility for FTIR analysis. The authors are grateful to Sophisticated Test and Instrumentation Centre (STIC), Cochin for providing facility to perform TEM analysis. We are also thankful to SRM University, Tamil Nadu for SEM and EDAX analysis. DST-PURSE program is kindly acknowledged for providing the CLSM facility to BDU.

6 References

[1] Rybtke, M., Hultqvist, L.D., Givskov, M., *et al.*: '*Pseudomonas aeruginosa* biofilm infections: community structure, antimicrobial tolerance and immune response', *J. Mol. Biol.*, 2015, **427**, (23), pp. 3628–3645

[2] Cole, S.J., Records, A.R., Orr, M.W., *et al.*: 'Catheter-associated urinary tract infection by *Pseudomonas aeruginosa* is mediated by exopolysaccharide-independent biofilms', *Infect. Immun.*, 2014, **82**, (5), pp. 2048–2058

[3] Wei, Q., Ma, L.Z.: 'Biofilm matrix and its regulation in *Pseudomonas aeruginosa*', *Int. J. Mol. Sci.*, 2013, **14**, (10), pp. 20983–21005

[4] Hoffman, J.R., Kang, J., Ratamess, N.A., *et al.*: 'Thermogenic effect of an acute ingestion of a weight loss supplement', *J. Int. Soc. Sports Nutr.*, 2009, **6**, p. 1

[5] Guven, K.C., Percot, A., Sezik, E.: 'Alkaloids in marine algae', *Mar. Drugs*, 2010, **8**, (2), pp. 269–284

[6] Sharma, G., Rao, S., Bansal, A., *et al.*: '*Pseudomonas aeruginosa* biofilm: potential therapeutic targets', *Biologicals*, 2014, **42**, (1), pp. 1–7

[7] Huang, X., Jain, P.K., El-Sayed, I.H., *et al.*: 'Gold nanoparticles: interesting optical properties and recent applications in cancer diagnostics and therapy', *Nanomedicine*, 2007, **2**, (5), pp. 681–693

[8] Manju, S., Malaikozhundan, B., Vijayakumar, S., *et al.*: 'Antibacterial, antibiofilm and cytotoxic effects of *Nigella sativa* essential oil coated gold nanoparticles', *Microb. Pathog.*, 2016, **91**, pp. 129–135

[9] Ahmed, A., Khan, A.K., Anwar, A., *et al.*: 'Biofilm inhibitory effect of chlorhexidine conjugated gold nanoparticles against *Klebsiella pneumoniae*', *Microb. Pathog.*, 2016, **98**, pp. 50–56

[10] Masak, J., Cejkova, A., Schreiberova, O., *et al.*: 'Pseudomonas biofilms: possibilities of their control', *FEMS Microbiol. Ecol.*, 2014, **89**, (1), pp. 1–14

[11] Ghosh, S., Patil, S., Ahire, M., *et al.*: 'Synthesis of gold nanoanisotrops using *Dioscorea bulbifera* tuber extract', *J. Nanomater.*, 2012, **7**, pp. 483–496

[12] Song, J.Y., Jang, H.K., Kim, B.S.: 'Biological synthesis of gold nanoparticles using *Magnolia kobus* and *Diopyros kaki* leaf extracts', *Process Biochem.*, 2009, **44**, (10), pp. 1133–1138

[13] Gopinath, K., Gowri, S., Karthika, V., *et al.*: 'Green synthesis of gold nanoparticles from fruit extract of *Terminalia arjuna*, for the enhanced seed germination activity of *Gloriosa superba*', *J. Nanostruct. Chem.*, 2014, **4**, p. 15

[14] Mukherjee, S., Sushma, V., Patra, S., *et al.*: 'Green chemistry approach for the synthesis and stabilization of biocompatible gold nanoparticles and their potential applications in cancer therapy', *Nanotechnology*, 2012, **23**, (45), p. 455103

[15] Payne, J.N., Waghwani, H.K., Connor, M.G., *et al.*: 'Novel synthesis of kanamycin conjugated gold nanoparticles with potent antibacterial activity', *Front. Microbiol.*, 2016, **7**, p. 607

[16] Li, Y., Li, Y., Li, Q., *et al.*: 'Rapid biosynthesis of gold nanoparticles by the extracellular secretion of *Bacillus niabensis* 45: characterization and antibiofilm activity', *J. Chem.*, 2016, **2016**, pp. 1–7, http://dx.doi.org/10.1155/2016/2781347

[17] Ansari, M.A., Khan, H.M., Khan, A.A., *et al.*: 'Gum arabic capped-silver nanoparticles inhibit biofilm formation by multi-drug resistant strains of *Pseudomonas aeruginosa*', *J. Basic Microbiol.*, 2014, **54**, (7), pp. 688–699

[18] Mary, R.N.I., Banu, N.: 'Screening of antibiofilm and anti-quorum sensing potential of *Vitex trifolia* in *Pseudomonas aeruginosa*', *Int. J. Pharm. Pharm.*, 2015, **7**, pp. 242–245
[19] Kalia, M., Yadav, V.K., Singh, P.K., *et al.*: 'Effect of cinnamon oil on quorum sensing-controlled virulence factors and biofilm formation in *Pseudomonas aeruginosa*', *PLoS ONE*, 2015, **10**, (8), p. e0135495
[20] Packiavathy, I.A.S.V., Agilandeswari, P., Musthafa, K.S., *et al.*: 'Antibiofilm and quorum sensing inhibitory potential of *Cuminum cyminum* and its secondary metabolite methyl eugenol against Gram negative bacterial pathogens', *Food Res. Int.*, 2012, **45**, pp. 85–92
[21] Wang, X., Yao, X., Zhu, Z., *et al.*: 'Effect of berberine on *Staphylococcus epidermidis* biofilm formation', *Int. J. Antimicrob. Agents*, 2009, **34**, (1), pp. 60–66
[22] Sujitha, M.V., Kannan, S.: 'Green synthesis of gold nanoparticles using citrus fruits (*Citrus limon*, *Citrus reticulata* and *Citrus sinensis*) aqueous extract and its characterization', *Spectrochim. Acta A Mol. Biomol. Spectrosc.*, 2013, **102**, pp. 15–23
[23] Islam, N.U., Jalil, K., Shahid, M., *et al.*: 'Green synthesis and biological activities of gold nanoparticles functionalized with *Salix alba*', *Arab. J. Chem.*, 2015, https://doi.org/10.1016/j.arabjc.2015.06.025
[24] Wang, Y., He, X., Wang, K., *et al.*: 'Barbated Skullcup herb extract-mediated biosynthesis of gold nanoparticles and its primary application in electrochemistry', *Colloids Surf. B Biointerfaces*, 2009, **73**, (1), pp. 75–79
[25] Chandran, S.P., Chaudhary, M., Pasricha, R., *et al.*: 'Synthesis of gold nanotriangles and silver nanoparticles using Aloe vera plant extract', *Biotechnol. Prog.*, 2006, **22**, pp. 577–583